

A mesoscale phase-field model of intergranular liquid lithium corrosion of ferritic/martensitic steels: COMSOL implementation

Alexandre Lhoest^a, Sasa Kovacevic^b, Duc Nguyen-Manh^c, Joven Lim^c, Emilio Martínez-Pañeda^{b,*}, Mark R. Wenman^a

^a*Imperial College London, Centre for Nuclear Engineering, South Kensington Campus, London SW7 2AZ, UK*

^b*Department of Engineering Science, University of Oxford, Oxford OX1 3PJ, UK*

^c*United Kingdom Atomic Energy Authority, Culham Campus, Abingdon OX14 3DB, UK*

Abstract

A phase-field model for simulating the intergranular corrosion of ferritic/martensitic steels exposed to liquid lithium is developed by Lhoest et al. (2025) [1]. The framework naturally captures the enhanced corrosion at the grain boundaries relative to the metal grain by exploiting the solid-state diffusivities of Cr. Further, the model highlights the synergy between microstructural features and corrosion performance of the material, thereby identifying key properties to guide the production of corrosion resistant materials.

The theoretical formulation of the phase-field model is provided in the original paper [1] while this document provides instructions for its implementation in the finite element software COMSOL Multiphysics. Input files for intergranular corrosion are provided for demonstration purposes. If the code developed is used for research or industrial purposes, please cite:

Lhoest, A., Kovacevic, S., Nguyen-Manh, D. et al., A mesoscale phase-field model of intergranular liquid lithium corrosion of ferritic/martensitic steels, *npj Mater Degrad* **9**, 68 (2025), <https://doi.org/10.1038/s41529-025-00616-4>.

Keywords: Diffuse interface, Grain boundary density, Corrosion damage, Solubility-driven dissolution, Cr depletion

*Corresponding authors

Email address: emilio.martinez-paneda@eng.ox.ac.uk (Emilio Martínez-Pañeda)

1. Mathematical formulation

This section briefly introduces the mathematical formulation of the phase-field model for the intergranular corrosion of ferritic/martensitic steels exposed to liquid lithium. The interested reader is referred to the original paper for more details [1].

The problem formulation is depicted in Fig. 1 and can be summarized as follows. The system domain Ω contains a polycrystalline steel specimen exposed to static liquid lithium. The spatial distribution of each phase and thus the evolution of the corroding interface is defined using a continuous phase-field parameter ϕ such that $\phi = 1$ denotes the solid phase (i.e., ferritic/martensitic steel) and $\phi = 0$ represents the liquid phase (i.e., liquid lithium) which are separated by a thin diffuse interfacial region defined as $0 < \phi < 1$. The liquid lithium is represented via a concentration sink on the upper most domain boundary Γ_{top} . The remaining three domain boundaries Γ_{left} , Γ_{bottom} , and Γ_{right} are prescribed zero Neumann boundary conditions to simulate a closed system. Grain boundaries (GBs) and metal grains are distinguished using a supplementary order parameter η such that $\eta = 1$ are applied to GBs that are expected to corrode with $\eta = 0$ applied elsewhere. Through this, two independent diffusion coefficients of Cr: GB D'_{gb} and metal grain D_{mg} , are exploited to isolate the corrosion at the GBs. In summation, two independent kinematic variables are employed to describe the corrosion process; the non-conserved phase-field order parameter $\phi(\mathbf{x}, t)$ and the normalized concentration of Cr $\bar{c}(\mathbf{x}, t) = c/c_{\text{solid}}$ which expresses the initial composition of the material plus the temporal chemical degradation.

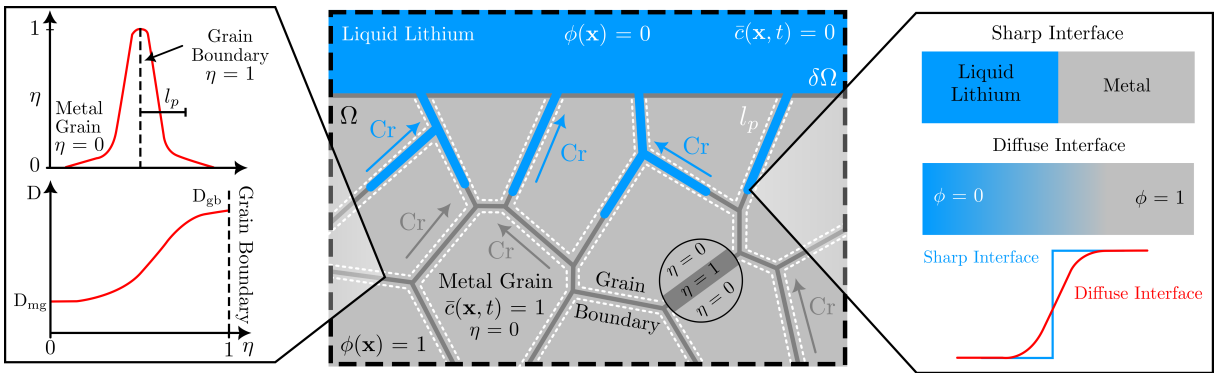


Figure 1: Polycrystalline material in contact with a corrosive environment highlighting the diffuse interface between the liquid ($\phi = 0$) and solid ($\phi = 1$) phases. The GBs possess a heightened diffusivity D_{gb} compared to the metal grain D_{mg} via an additional parameter that differentiates between GB ($\eta = 1$) and metal grain ($\eta = 0$). The corrosion mechanism is based on the bulk diffusion of Cr towards the exposed surface.

The free energy functional that describes the heterogeneous systems in Fig. 1 can be expressed

as

$$\mathcal{F} = \int_{\Omega} [f^{\text{chem}}(\bar{c}, \phi) + f^{\text{grad}}(\nabla \phi)] d\Omega, \quad (1)$$

where f^{chem} and f^{grad} denote the chemical and gradient energy densities, respectively, as defined below.

1.1. Chemical free energy density

The chemical free energy density is expressed as the weighted sum of free energy density from each contributing phase

$$f^{\text{chem}}(\bar{c}, \phi) = h(\phi) f_s^{\text{chem}}(\bar{c}_s) + (1 - h(\phi)) f_l^{\text{chem}}(\bar{c}_l) + \omega g(\phi), \quad (2)$$

where $f_s^{\text{chem}}(\bar{c}_s)$ and $f_l^{\text{chem}}(\bar{c}_l)$ are the chemical free energy densities with respect to the normalized concentrations in the liquid (\bar{c}_l) and solid (\bar{c}_s) phases. $g(\phi) = 16\phi^2(1 - \phi)^2$ is the double-well free energy function employed to describe the two equilibrium states for the solid ($\phi = 1$) and the liquid ($\phi = 0$) phases. ω is the constant that determines the height of the energy barrier at $\phi = 1/2$ between the two minima at $\phi = 0$ and $\phi = 1$. $h(\phi) = \phi^3(6\phi^2 - 15\phi + 10)$ is a monotonously increasing interpolation function that interpolates the chemical free energy density between the two phases. The chemical free energy density of each phase can be reasonably approximated by a simple parabolic function around equilibrium concentrations with the same free energy density curvature parameter A as

$$f_s^{\text{chem}}(\bar{c}_s) = \frac{1}{2} A (\bar{c}_s - \bar{c}_{s,\text{eq}})^2 \quad f_l^{\text{chem}}(\bar{c}_l) = \frac{1}{2} A (\bar{c}_l - \bar{c}_{l,\text{eq}})^2, \quad (3)$$

where $\bar{c}_{s,\text{eq}} = c_{\text{solid}}/c_{\text{solid}} = 1$ and $\bar{c}_{l,\text{eq}} = c_{\text{sat}}/c_{\text{solid}}$ are the normalized equilibrium concentrations for the solid and liquid phase. Here, c_{sat} represents the saturation limit of the metal species in the liquid phase. Each material point in the present model is characterized as a mixture of both solid and liquid phases with different compositions yet the same diffusion chemical potentials. This assumption renders the following expression for the chemical free energy density $f^{\text{chem}}(\bar{c}, \phi)$

$$f^{\text{chem}}(\bar{c}, \phi) = \frac{1}{2} A [\bar{c} - h(\phi)(\bar{c}_{s,\text{eq}} - \bar{c}_{l,\text{eq}}) - \bar{c}_{l,\text{eq}}]^2 + \omega g(\phi). \quad (4)$$

1.2. Gradient free energy density

The gradient free energy density is commonly expressed as

$$f^{\text{grad}}(\nabla\phi) = \frac{1}{2}\kappa|\nabla\phi|^2 \quad (5)$$

where κ is the isotropic gradient energy coefficient. The phase-field parameters ω in Eq. (2) and κ in Eq. (5) are connected to the interfacial energy Γ and the chosen nominal interface thickness ℓ as

$$\kappa = \frac{3}{2}\Gamma\ell \quad \omega = \frac{3\Gamma}{4\ell}. \quad (6)$$

1.3. Governing equations

The following time-dependent governing equations for the independent kinematic fields $\phi(\mathbf{x}, t)$ and $\bar{c}(\mathbf{x}, t)$

$$\left\{ \begin{array}{l} \frac{\partial\phi}{\partial t} = -L\left(\frac{\partial f^{\text{chem}}}{\partial\phi} - \kappa\nabla^2\phi\right) \\ \frac{\partial\bar{c}}{\partial t} = -\nabla \cdot \mathbf{J}; \quad \mathbf{J} = -D\nabla\bar{c} - Dh'(\phi)(\bar{c}_{l,eq} - \bar{c}_{s,eq})\nabla\phi \end{array} \right\} \quad \text{in } \Omega, \quad (7)$$

complemented with boundary conditions

$$\kappa\mathbf{n} \cdot \nabla\phi = 0 \quad \text{and} \quad \mathbf{n} \cdot \mathbf{J} = 0 \quad \text{on} \quad \partial\Omega. \quad (8)$$

In addition, Dirichlet boundary conditions for both ϕ and \bar{c} equating to zero are prescribed on the upper most boundary Γ_{top} implemented via a step function to improve numerical stability. The interface kinetic coefficient in Eq. (7) defines the interfacial mobility and D is the effective diffusion coefficient of Cr composition which is further broken down to encapsulate the GB diffusivity D_{gb} and metal grain diffusivity D_{mg} of Cr, such that $D_{\text{gb}} \gg D_{\text{mg}}$ is enforced.

$$D = D'_{\text{gb}}\eta + (1 - \eta)D_{\text{mg}} \quad D'_{\text{gb}} = \frac{\delta_{gb}}{l_p}D_{\text{gb}}. \quad (9)$$

Herein, D'_{gb} is the effective diffusion coefficient of Cr along GBs and is the result of the constant product approach. Consequentially, the GB diffusivity D_{gb} is proportionally altered with respect to the thickness of the Cr depletion at the GBs. This is achieved by taking the product with the ratio of the experimentally determined physical Cr depletion thickness δ_{gb} and the simulated thickness of the smeared GB region l_p . The interpolation of GBs is managed via the static order

parameter η given as

$$\nabla \cdot (-l_p^2 \nabla \eta) + \eta = 0 \quad \text{in } \Omega, \quad (10)$$

accompanied with boundary conditions

$$l_p^2 \mathbf{n} \cdot \nabla \eta = 0 \quad \text{on } \partial\Omega \quad \text{and} \quad \eta = 1 \quad \text{on GBs.} \quad (11)$$

2. COMSOL implementation

The Voronoi tessellations used to mimic the steels microstructures are generated using a custom MATLAB script applied through LiveLink for MATLAB. This procedure imports the generated Voronoi diagram as a geometry in a COMSOL file which is later exported to use accordingly. The custom script allows for the dimensions of the computational domain as well as the number of grains to be altered with ease. In conjunction, these parameters are chosen to yield a desired microstructure via the equivalent diameter method. In this study a 100 μm by 100 μm was chosen with a reference average grain size of 20 μm , Fig. 2.

The governing equations, Eq. (7) and (10), are implemented into COMSOL using appropriate PDE mathematical forms along with the corresponding boundary conditions, Eq. (8). The Dirichlet boundary condition in Eq. (11) applies only to GBs that are expected to corrode to save computational expense due to meshing, as further detailed in the next section. The initial values of ϕ and \bar{c} are equal to unity whereas η is equal to zero, Fig. 2. The employed physical and computational parameters used are found in Table 1.

Table 1: Material and computational parameters employed in the model.

Parameter	Value	Unit
Chemical free energy density curvature parameter A	5×10^9	N/m ²
Interface kinetics coefficient L	1	m ² /(N.s)
Concentration in the solid phase c_{solid}	13.4	mol/L
Saturated concentration in the liquid phase c_{sat}	10.3	mol/L
Interfacial energy Γ	4	N/m
Computational GB thickness l_p	100	nm
Physical Cr depletion thickness δ_{gb}	15	nm
Interfacial thickness ℓ	4	μm
Grain boundary diffusivity D_{gb}	1.70×10^{-15}	m ² /s
Metal grain diffusivity D_{mg}	5.11×10^{-21}	m ² /s

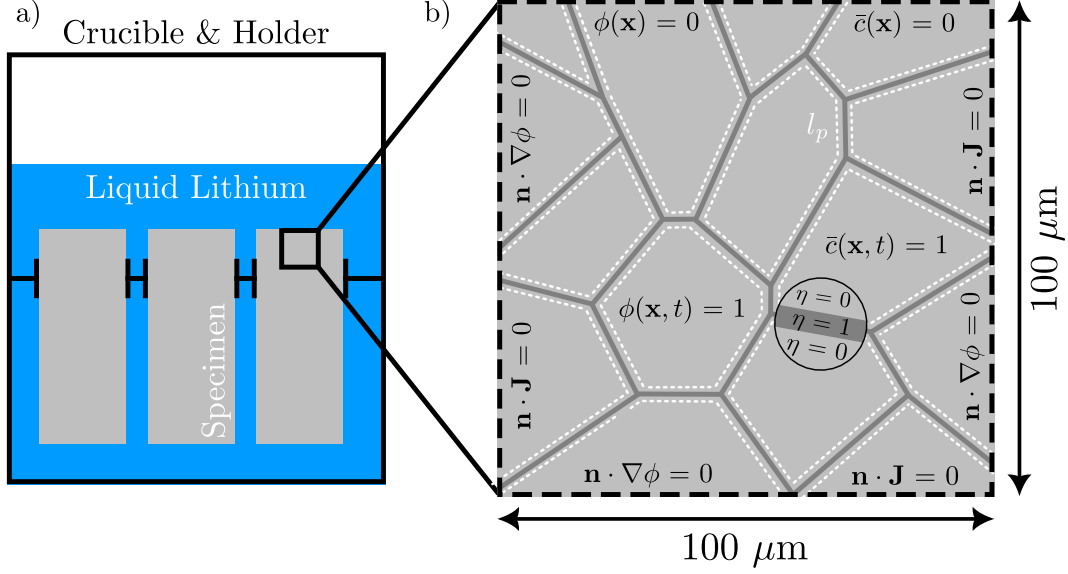


Figure 2: Schematic of the (a) experimental apparatus to expose ferritic/martensitic specimen to static liquid lithium and (b) corresponding computational domain consisting of a polycrystalline material with the initial values and boundary conditions. The exposed surface is the upper most boundary.

3. Numerical implementation

The framework developed is implemented into the multi-purpose finite element software package COMSOL Multiphysics [2]. The computational domain is discretized using triangular finite elements with second-order Lagrangian interpolation functions. All regions expected to corrode in the metal grains are given a characteristic maximum element size at least five times smaller than the interfacial thickness ℓ to ensure a smooth transition between the metal and corrosive agent. Moreover, as the evolution of the interface is expected to be most prominent at the GBs compared to the metal grain, a maximum element size of $\ell/20$ is applied to all GBs which possess $\eta = 1$. Finally, to limit the computational cost, the remaining domain of the solid phase is given a maximum element size of ℓ . Each simulation consists of a two-step study. The governing equation (10) for the interpolating parameter η that defines the smeared GB thickness is solved in the first step using a steady-state (time-independent) solver. The governing equations (7) for the evolution of the phase-field parameter ϕ and Cr composition \bar{c} are then solved in the second step using a time-dependent study. An implicit time-stepping method is used for temporal discretization in the time-dependent step. A fully coupled solution algorithm is selected to solve the governing equations. The maximum time step is 2 hours. The solver accuracy in each time step is controlled by a relative tolerance of 10^{-4} .

4. Conclusions

A finite element implementation of the phase-field model for simulating the intergranular corrosion of ferritic/martensitic steels when exposed to liquid lithium developed by Lhoest et al. (2025) is presented. The present document provides details of the model implementation in the software package COMSOL Multiphysics. The code developed is freely available at <https://mechmat.web.ox.ac.uk/codes>.

References

- [1] A. Lhoest, S. Kovacevic, D. Nguyen-Manh, J. Lim, E. Martínez-Pañeda, M. R. Wenman, A mesoscale phase-field model of intergranular liquid lithium corrosion of ferritic/martensitic steels, npj Materials Degradation 9 (1) (2025) 68. doi:10.1038/s41529-025-00616-4.
- [2] COMSOL Multiphysics v. 6.0. <https://www.comsol.com>. COMSOL AB, Stockholm, Sweden.